Int J Adv Manuf Technol (2015) 79:1117–1126
DOI 10.1007/s00170-015-6893-9

ORIGINAL ARTICLE

An investigation on distortion of PLA thin-plate part in the FDM process

Liu Xinhua · Li Shengpeng · Liu Zhou · Zheng Xianhua · Chen Xiaohu · Wang Zhongbin

Received: 17 August 2014 / Accepted: 9 February 2015 / Published online: 26 February 2015

Abstract In order to reveal the distortion mechanism of PLA thin-plate part in the FDM process, a theoretical model based on the theory of elastic thin plates in thermoelasticity was established, and an experimental research approach based on Taguchi method was presented. A special specimen was designed, and the flowchart of experimental procedure was elaborated. Moreover, 81 test specimens were prepared through FDM process and measured by a portable 3D laser scanner. Two statistical analysis methods, signal to noise ratio (S/N) and analysis of variance (ANOVA), were applied to optimize the process parameters in order to reduce the distortion of thin-plate part. The experimental results indicated that the optimal process parameters can be obtained and proposed theoretical model was proved efficient.

Keywords Fused deposition modeling · Thin-plate part distortion · Polylactic acid (PLA) · Taguchi method

1 Introduction

As a manufacturing technology to fabricate physical models or parts rapidly, rapid prototyping technology (RPT) is widely applied in the machinery, aerospace, construction, medical, cultural, and other fields [1–3]. Under the computer control and management, RPT manufactures part using accurate accumulation of materials relying on the existing CAD model. Different from traditional machining methods, RPT adopts the additive manufacturing processes [4]. The representative processes of RPT are fused deposition modeling (FDM), stereolithography apparatus (SLA), laminated object manufacturing(LOM), selective laser sintering(SLS), 3D printing(3DP), etc.

In FDM process, the hot-melting filament feedstock (ABS, PLA, Polyamides, low-melting-point metal, etc.) are heated up to their melting point temperature and then deposited by an extrusion head; meanwhile, the extrusion head can be moved in both horizontal and vertical directions by a numerically controlled mechanism. The nozzle follows a tool-path which is controlled by computer-aided manufacturing (CAM) software, and the part is built from the bottom up, one layer at a time [5, 6]. In recent years, the development of low-cost desktop 3D printer, such as MakerBot, RepRap, Fab@Home, and Cube etc, has made FDM process widely accessible for producing highly individual products for individual needs and small-scale manufacturing part in home and office. Most desktop 3D printers currently adopt either acrylonitrile butadiene styrene (ABS) or polylactic acid (PLA) as modeling materials. Due to the inferior thermostability, ABS would resolve into acrylonitrile-monomer, butadiene-monomer, and styrene-monomer when it is heated up to 250 °C. As we all known, the acrylonitrile is an extremely toxic substance [7]. However, the PLA can be degraded into H_2O, CO_2, and humus; so, it is an ideal green polymer material and also can be highly versatile, biodegradable, aliphatic polyester produced from reproducible resources, such as corn and cassava [8]. Besides, the PLA filament has a low-cost, low-melting point, and high mechanical property than ABS filament [9, 10]. Based on the above advantages, the PLA filament is largely used in the FDM process.

As one of the most difficult problems in the FDM process, part distortion almost cannot be avoided. The hot-melting feedstock has experienced the glassy state, high elastic state, and

L. Xinhua · L. Shengpeng · L. Zhou · Z. Xianhua · C. Xiaohu · W. Zhongbin
School of Mechanical and Electrical Engineering, China University of Mining and Technology, Xuzhou, China

L. Xinhua (✉)
Xuyi Mine Equipment and Materials R&D Center, China University of Mining and Technology, Huai'an, China
e-mail: l_xinhua_2006@126.com

viscous state during the deposition process. This phase change process is characterized by the accumulation of residual stresses and strains during material building up [11].When accumulated to a certain extent, the residual stress would lead to distortion and cracking in the part, which seriously affects the molding quality.

The rest of this paper is organized as follows: Some related works are outlined based on literature in Sect. 2. Theoretical model of PLA thin-plate part distortion is presented in Sect. 3. The experimental research is proposed in Sect. 4. The experimental results and discussion are elaborated in Sect. 5. The conclusions and future work are summarized in Sect. 6.

2 Literature review

Aiming at investigating the distortion of molding part, lots of theoretical models had been established. In the study of Wang et al. [12], they constructed a mathematical model for warp deformation of the part according to fundamental hypotheses and simplifications. The authors quantificationally analyzed the effects of deposition layer number, the stacking section length, the chamber temperature, and the material linear shrinkage rate for warp deformation. In Vatani et al. [13], they developed a model to predict the distortion of SLA parts based on classical lamination theory. The authors found that the final distortion increased exponentially when layer thickness decreased. Similar work had been done by Kim et al [14]. In Yan et al. [15], they established a simple model for the laminated object manufacturing process and considered that the equivalent bending moment caused by internal stress was the basic reason of part distortion. In Xu et al. [16], they proposed a mechanical equivalent model of resin phase change shrinkage in stereolithography in accordance with the distortion mechanism of thin plate. Based on this model, the authors presented the numerical simulation of part distortion in SLA using the commercial package ABAQUS.

Numerical analysis methods had been adopted to simulate residual stresses in RPT. In Jayanthi et al. [17], they developed a dynamic finite element simulation model to simulate the photo polymerization of stereolithography process and researched the effect of scanning pattern of the laser for part distortion. In Wiedemann et al. [18], they researched the interaction between material properties and process parameters for part distortion in stereolithography through numerical simulation method. The authors stated that process parameters must be optimized to cater the individual material to reduce internal stresses in the part. In Dalgarno et al. [19], they developed a finite element model of part in the SLS process and discovered that adopting double sintering to the first two layers can reduce the part distortion. In Sonmez et al. [20], they developed a numerical analysis model for the thermomechanical behavior of a laminate during the LOM process to study stress distributions and distortion phenomena in the laminate. Similar finite element analysis model had been developed by Nickel et al. and Zhang and Chou [21, 22].

In addition, some process measures to avoid distortion phenomenon in RPT had been proposed by many researchers. In Yugang et al. [23], they explained the distortion of part manufactured by laser rapid prototyping from resin microstructure and distortion mechanism and suggested that improved properties of the resin and scanning pattern could reduce the distortion. In Wanhua et al. [24], they proposed a new filling pattern called separate area scanning to reduce the part deformation in SLA process. In Yang et al. [25], they proposed a compensation method for the distortion of the SLS parts. In Mahesh et al. [26], they designed a benchmark part to evaluate several RPT processes. The authors discovered that the thermal cycling of the materials lead to asymmetrical thermal gradients which caused residual stress resulting in distortion. In Buchbinder et al. [27], they reduced the distortion of aluminum components fabricated by selective laser melting using preheating method.

Although many theoretical models, numerical analysis methods, and process measures have been proposed to reduce the distortion of RPT part in above literature, they have some common disadvantages summarized as follows. First, most of previous researchers have mainly studied the distortion mechanism of part fabricated by ABS, rare work has been done for PLA. Second, the previous theoretical models are difficult to predict the part distortion accurately, for example, the biggest distortion of thin-plate part occurs at its four corners. Finally, a systematic experimental study has not been done to provide the optimum combination of process parameters for minimum distortion. Based on our past research on the part distortion in the FDM process, this paper tries to tackle the above problems.

In this paper, a theoretical model based on the theory of elastic thin plates in thermoelasticity is established to predict the distortion of PLA thin-plate part, and an experimental research approach based on Taguchi method is proposed to optimize the process parameters of minimum distortion.

3 Theoretical model of PLA thin-plate part distortion

In order to formulate the problem in mathematical expression, the following notations are introduced first:

E	Elasticity modulus
ν	Poisson's ratio
α	Linear thermal coefficient of expansion
ε	Normal strain
γ	Shearing strain
T_m	Melting temperature
T_g	Glass transition temperature
T_e	Environment temperature
$T(x,y,z)$	Temperature gradient function

δ	Thickness of thin-plate part
δ_0	Layer thickness
n	The number of layers
D	Bending stiffness
∇^2	Laplace operator
w	Deflection (characterizing the distortion of thin-plate part)
q_{Teq}	Equivalent transverse load
n	Equivalent bending moment

3.1 Fundamental assumptions

Before establishing the theoretical model of PLA thin-plate part distortion, it is necessary to simplify the depositing process. The fundamental assumptions and simplifying items are presented as follows.

1. The PLA filament feedstock has a weak ability to resist the external force in the cooling process from T_m to T_g, which results in the filament occurring a larger shrinking with less force. Therefore, there is no internal stress accumulated in the part during this process. The internal stress in the part is mainly produced from T_g to T_e.
2. The high-temperature filament cools below T_g in a extremely short time [12].
3. In order to facilitate the analysis, it is considered that each layer has been deposited instantaneously, i.e., the temperature is a constant within the same layer; the molding and shrinking of filament feedstock proceed synchronously in a layer.
4. There is a pair of contractile force between adjacent two layers, and it is a nonuniform surface force. The contractile force can be decomposed orthogonally to the normal stress component and shear stress component, and the normal stress is perpendicular to the plane, and the shear stress is parallel to the plane, the direction points toward a shrinking center, as shown in Fig. 1.
5. The deposited PLA thin-plate part is regarded as the isotropic body [28].

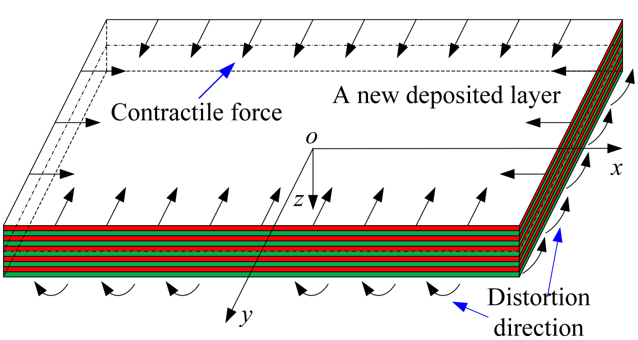

Fig. 1 The schematic diagram of theoretical model

3.2 The theoretical model for the distortion of PLA thin-plate part

If an element in the elastomer is unconstrained, a normal strain, equaling to αT, would be caused by temperature gradient T. Based on assumption 5 and the thermal elasticity theory [29], the distortion component of the element in the isotropic elastomer can be calculated as follows:

$$\begin{cases} \varepsilon_x = \varepsilon_y = \varepsilon_z = \alpha T \\ \gamma_{xy} = \gamma_{yz} = \gamma_{zx} = 0 \end{cases} \quad (1)$$

Based on assumption 3, it can be found that the temperature gradient T is the difference of planar temperature field between two adjacent layers, and it only changes with the z; therefore, the issue can be reduced to two-dimensional thermal stress problem. According to the equivalent relationship between temperature load and mechanical load in the thermal elasticity theory [29], the displacement caused by temperature gradient T is equal to the displacement caused by the following virtual external forces.

The volume force component f_{Vx} and f_{Vy} can be calculated as follows:

$$\begin{cases} f_{Vx} = -\dfrac{E\alpha}{1-\nu}\cdot\dfrac{\partial T}{\partial x} \\ f_{Vy} = -\dfrac{E\alpha}{1-\nu}\cdot\dfrac{\partial T}{\partial y} \end{cases} \quad (2)$$

The normal surface stress σ_N can be calculated as follows:

$$\sigma_N = -\frac{E\alpha T}{1-\nu} \quad (3)$$

As shown in Fig. 2, at any point in the thin-plate part, the temperature gradient function $T(x,y,z)$ can be expressed as follows:

$$T(x,y,z) = T(z) = \begin{cases} T_g - T_e & (n-1)\delta_0 - \delta/2 \le z \le \delta/2 \\ 0 & -\delta/2 \le z \le (n-1)\delta_0 - \delta/2 \end{cases} \quad (4)$$

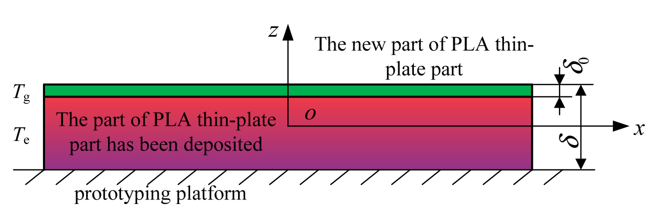

Fig. 2 A PLA thin-plate part

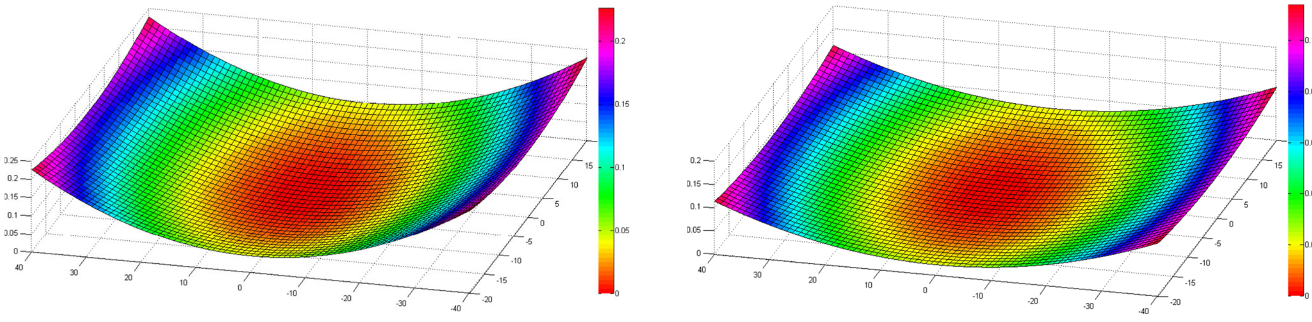

(a) The $50th$-layer (b) The $100th$-layer

Fig. 3 Deflection of $50th$-layer and $100th$-layer

The differential equation for solving bending problem of thin plate under the thermal stress can be presented as follows [30].

$$D\nabla^4 w = q_{Teq} = \nabla^2 M_{Teq} \quad (5)$$

where $D = \frac{E\delta^3}{12(1-\nu^2)}$, $\nabla^2 = \frac{\partial^2}{\partial x^2} + \frac{\partial^2}{\partial y^2}$, $\nabla^4 = (\nabla^2)^2$, $q_{Teq} = -\frac{E\alpha}{(1-\nu)} \int_{-\delta/2}^{\delta/2} \nabla^2\, T(x,y,z) z dz$, $M_{Teq} = -\frac{E\alpha}{(1-\nu)} \int_{-\delta/2}^{\delta/2} T(x,y,z) z dz$.

When temperature gradient function $T(x,y,z)=T(z)$ and thin-plate borders are all free, the solution of Eq. (5), deflection of thin plate, can be shown as follows:

$$w(x,y) = \frac{6\alpha\left(T_g - T_e\right)(2n-1)(1+\nu)}{\delta_0 n^3}\left(x^2 + y^2\right) \quad (8)$$

The Eq. (8) is the computational formula for the deflection of PLA thin-plate part fabricated by the FDM process.

The following conclusions can be obtained from the established theoretical model.

1. The biggest deflection of PLA thin-plate part occurs at its four corners.
2. With the increasing of deposition layers, the deflection caused by the current layer shrinking shows the trend of decreasing, i.e., the distortion mainly occurs in the initiative several layers. Figure 3 illustrates the deflection of $50th$-layer and $100th$-layer fitted by Matlab 2012 using the Eq. (8).

Through observing Fig. 3, it can be found that there is a shrinking center in the deposition layer. The deflection is smaller near shrinking center, and the greater is the farther from it.

4 The experimental research approach

4.1 Process parameter selection

Based on the theory analysis above-mentioned and previous research results [12, 23], the five major process parameters, such as the layer thickness, filling speed, nozzle temperature, filling style, and raster width, are investigated in this paper. The values of each level for these factors are selected according to value recommended by the equipment manufacturer,

Table 1 Control factors and their levels

Factors	Symbol	Unit	Level		
			low (1)	medium (2)	high (3)
Layer thickness	A	mm	0.3	0.2	0.1
Filling speed	B	mm/s	70	90	110
Nozzle temperature	C	degrees centigrade	220	230	240
Filling style	D	—	short raster	long raster	offset raster
Raster width	E	mm	0.3	0.4	0.5

past experiences, and real applications as shown in Table 1 and defined as follows [31].

1. Layer thickness: It is the thickness of layer deposited by nozzle and depends upon the type of nozzle used.
2. Filling speed: It is the travelling speed of nozzle when it fills a layer of part. This factor influences the heating and cooling frequency in the process of deposition, which affects residual stresses in the part [18].
3. Nozzle temperature: It is the temperature of nozzle when it works normally. This factor mainly affects the heat inputted into system in a specific period of time.
4. Filling style: It is the pattern of raster used to fill the interior regions of the PLA thin-plate part. The schematic diagram of three typical filling styles, which are short-raster, long-raster, offset-raster, mentioned in this paper are exhibited in Fig. 4.
5. Raster width: It is the width of raster pattern which refers to the width of the deposition path related to tip size [32].

Other factors are kept at their fixed level as shown in Table 2.

4.2 Specimen preparation

A special test specimen is designed in this paper, and its shape and dimensions are shown in Fig. 5, all units used are millimeter. The CAD model of specimen is modeled in Pro/ENGINEER Wildfire 5.0 and exported as a Standard Template Library (STL) file. Whereafter, the STL file is imported to the FDM software to form date files. The specimens for each experiment are fabricated using the Desktop 3D Printer MakerBot Replicator 2, and the filament feedstock used for fabricating test specimen is polylactic acid (PLA) mentioned in Sect. 1.

In order to fabricate the PLA thin-plate part accurately, the support structures are adapted as shown in Fig. 5a. Meanwhile, these structures can make the test specimen separated from prototyping platform easily by special heating-wire cutting tool as shown in Fig. 6 so as to reduce the effect of peeling force for the distortion of test specimen. In addition, the base structure is attached to be convenient for measurement subsequently. It is necessary to state that the support and base structure would increase redundant stiffness for test specimens and their influence on the distortion is not taken into consideration in this paper.

Table 2 Fixed factors and their levels

Fixed factors	Level	Unit
Build orientation	0	degree
Air gap	0	mm
Environment temperature	25	degrees centigrade
Visible surface	Normal raster	—
Number of shells	2	—
Infill	100 %	—

4.3 Experimental procedure

If the classical design of experiment (DOE) method is used to experimental design, it would require a total of 3^5 (243) experimental runs. Obviously, it is not practical and meaningful. Instead of the classical design of experiment method, the Taguchi method is adopted with lesser number of experimental runs in this paper [33].

In Taguchi design, an appropriate orthogonal array is very important for experiment. On the basis of our theoretical model for the distortion of PLA thin-plate part mentioned in the Sect. 3.2 and previous research results, it can be obtained that the layer thickness is an important factor for part distortion [12, 13, 22]. Therefore, the interactions between layer thickness with filling speed, nozzle temperature, and filling style are taken into account in this paper. Because five factors at three different levels and three interactions are considered, the total degree of freedom happens to be 26. Hence, the orthogonal array L_{27} (3^{13}) is selected for our experiment, which is

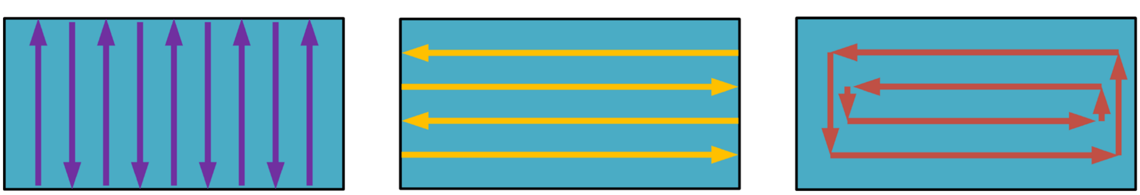

(a) short-raster (b) long-raster (a) offset-raster

Fig. 4 The schematic diagram of three typical filling styles

Fig. 5 Test specimen for the distortion of PLA thin-plate part

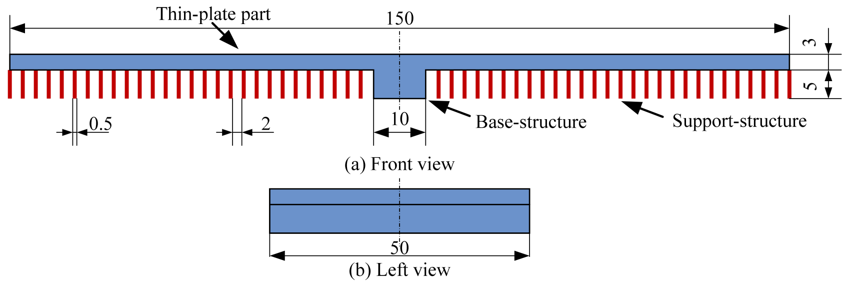

consisted of 13 columns for assigning factors and interactions and 27 rows for different experiment conditions. The final experimental plan is shown in Table 3. It is obvious that the experimental runs can be cut down from 243 to 27 by adopting the Taguchi method.

The flowchart of experimental procedure is shown in Fig. 6. In order to reduce the influence of accidental factors as much as possible, three identical test specimens are fabricated for each case, which resulted in a total of 81 test specimens. The noncontact measurement system, a portable 3D laser scanner, is used to measure experimental results to avoid the error caused by contact measurement such as the forces upon the test specimen influencing the accuracy. All the point cloud data acquired

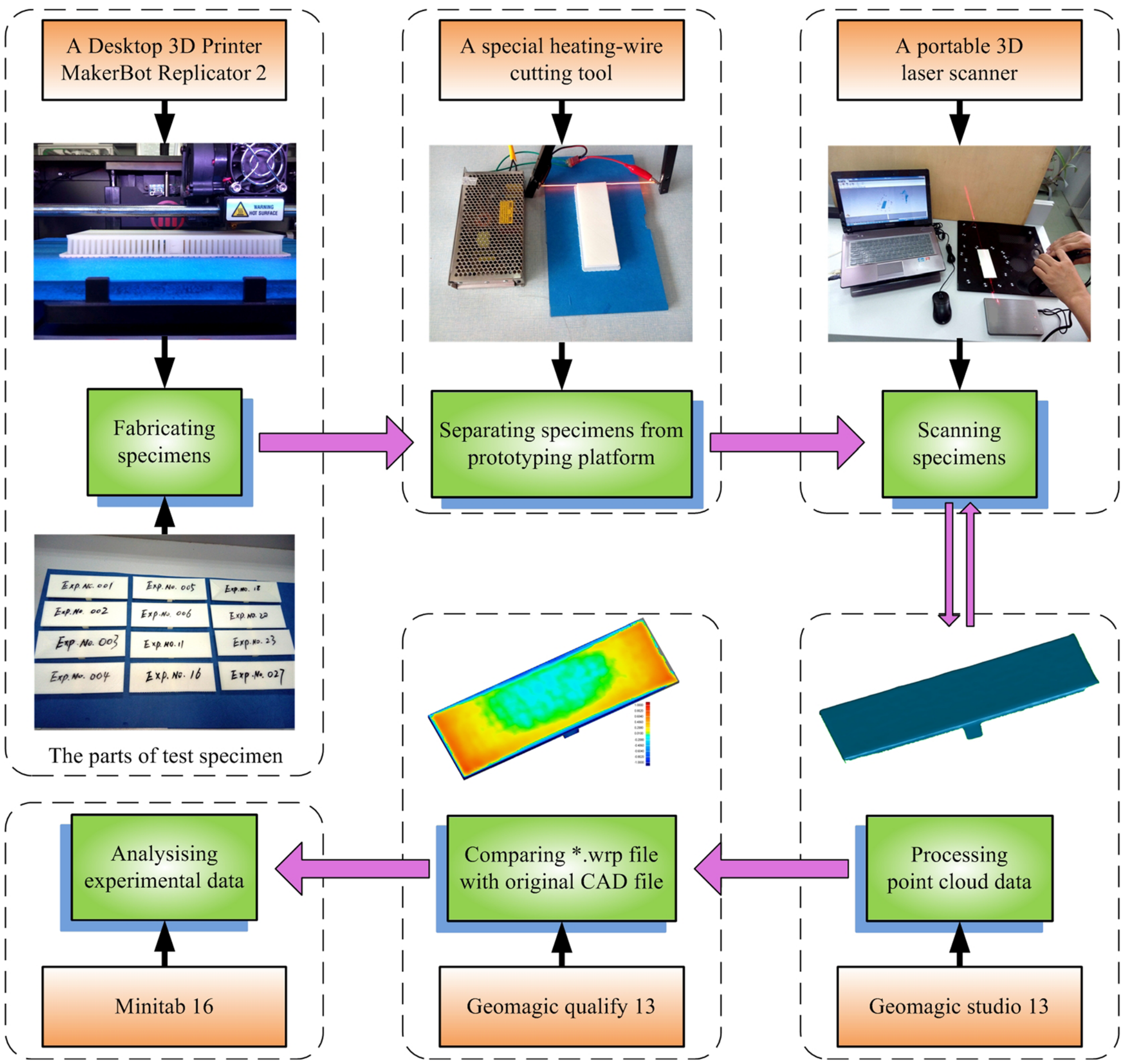

Fig. 6 The flowchart of experimental procedure

Table 3 Experimental plan with the average experimental data and S/N ratio data

Exp. no.	Factor					w_{ave} (mm)	S/N ratio (dB)
	A	B	C	D	E		
1	1	1	1	1	1	0.56	5.03624
2	1	1	2	2	2	0.77	2.27019
3	1	1	3	3	3	0.73	2.73354
4	1	2	1	2	3	0.76	2.38373
5	1	2	2	3	1	0.58	4.73144
6	1	2	3	1	2	0.58	4.73144
7	1	3	1	3	2	0.45	6.93575
8	1	3	2	1	3	0.38	8.40433
9	1	3	3	2	1	0.53	5.51448
10	2	1	1	1	1	0.82	1.72372
11	2	1	2	2	2	0.89	1.01220
12	2	1	3	3	3	0.85	1.41162
13	2	2	1	2	3	0.87	1.20961
14	2	2	2	3	1	0.71	2.97483
15	2	2	3	1	2	0.78	2.15811
16	2	3	1	3	2	0.66	3.60912
17	2	3	2	1	3	0.68	3.34982
18	2	3	3	2	1	0.89	1.01220
19	3	1	1	1	1	0.88	1.11035
20	3	1	2	2	2	1.21	−1.65571
21	3	1	3	3	3	0.97	0.26457
22	3	2	1	2	3	1.03	−0.25674
23	3	2	2	3	1	0.82	1.72372
24	3	2	3	1	2	1.14	−1.13810
25	3	3	1	3	2	0.75	2.49877
26	3	3	2	1	3	0.94	0.53744
27	3	3	3	2	1	0.98	0.17548

through the 3D laser scanner is processed using Geomagic studio 13 to obtain the *.wrp file. Then, comparing *.wrp file with original CAD file of test specimen using Geomagic qualify 13, the deflection of specimens would be obtained. What needs to stress, the average value of maximum deflection at four corners would be defined as observed value in this paper.

4.4 Analysis method for experimental results

In the Taguchi method, the signal to noise ratio (S/N) is adopted to evaluate the deviation between the experimental value and the ideal value. There are three quality characteristics in the analysis of the signal to noise ratio, such as the smaller-the-better characteristic, the nominal-the-better characteristic, and the larger-the-better characteristic. The objective of this paper is to reduce the distortion of PLA thin-plate part; therefore, the smaller-the-better characteristic is selected. Its signal to noise ratio (S/N) can be calculated as follows:

$$\eta = -10\log\left[\frac{1}{p}\sum_{i=1}^{p} w_i^2\right] \tag{10}$$

where p is the repeated times of each case, w_i is the value for current experiment.

Furthermore, the analysis of variance (ANOVA) can be adopted to identify the degree of importance of factors and interactions to the distortion of test specimens. The following equation can be used to calculate the parameters for ANOVA.

The total sum of square deviation (SST) and total degree of freedom (f_T) can be calculated as follows:

$$SST = \sum_{i=1}^{n} \eta_i^2 - \frac{T^2}{n} \tag{11}$$

$$f_T = n-1 \tag{12}$$

The sum of square deviation of j-th factor (SS_j) and its degree of freedom (f_j) can be calculated as follows:

$$SS_j = \frac{1}{r}\sum_{i=1}^{m} T_i^2 - \frac{T^2}{n} \quad (j = 1, 2, \cdots k) \tag{13}$$

$$f_j = m-1 \tag{14}$$

The sum of square of error (SSE) and its degree of freedom (f_e) can be calculated as follows:

$$SSE = SST - \sum_{j=1}^{k} SS_j \tag{15}$$

$$f_e = f_T - \sum_{j=1}^{k} f_j \tag{16}$$

The variance of j-th parameter (MS_j) and the variance of error (MSE) can be calculated as follows:

$$MS_j = SS_j/f_j \tag{17}$$

$$MSE = SSE/f_e \tag{18}$$

F-ratio of j-th factor can be calculated as follows:

$$F_j = MS_j/MSE \tag{19}$$

where n is the total number of experiments, m is the number of level for each factor, k is the number of columns of orthogonal array, $r=n/m$, T is the total sum of S/N ratio, T_i is the sum of S/N ratio when the level of factors is fixed on i-th row for an arbitrary column.

5 Experimental results and discussion

The main effect plot for signal to noise ratio, as shown in Fig. 7, is used to reflect the effect law of each factor for the distortion of test specimens, and the ANOVA results are presented in Table 4. Figure 8 presents two examples of error cloud chart between test specimen and CAD model (case 6, 20).

Table 4 Analysis of variance (ANOVA) table

Source	DOF	Sum of square	Variance	F-value	P
A	2	88.1250	44.0625	105.18	0.000
B	2	19.7318	9.8659	23.55	0.006
C	2	3.6089	1.8044	4.31	0.101
D	2	16.1307	8.0654	19.25	0.009
E	2	1.0625	0.5312	1.27	0.375
A*B	4	7.4163	1.8541	4.43	0.089
A*C	4	1.5689	0.3922	0.94	0.525
A*D	4	5.5399	1.3850	3.31	0.137
Error	4	1.6757	0.4189	—	—
Total	26	144.8596	—	—	—

The influence of five main factor levels on the distortion of PLA thin-plate part can be obtained intuitively from the main effect plot for S/N ratio and the optimum factor levels listed in Table 5. By the analysis of variance, the significant factors and interactions can be identified obviously, and the importance of factors and interactions for distortion of thin-plate part can be ranked as follows: A>B>D>A*B>C>A*D>E>A*C, and this result corresponds to main effect plot.

Comprehensive analysis of theoretical model and the experimental results, the conclusions can be summarized as follows:

1. By the statistical analysis of this experiment, it can be found that with the decreasing of layer thickness, the distortion of PLA thin-plate part increases obviously, and it is the most significant factor to the distortion. Meanwhile,

Fig. 7 Main effect plot for S/N ratio

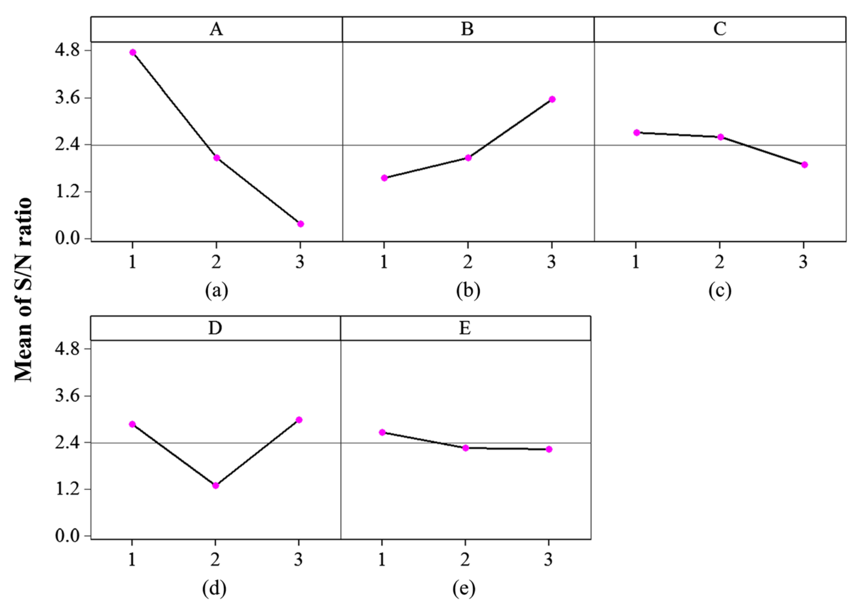

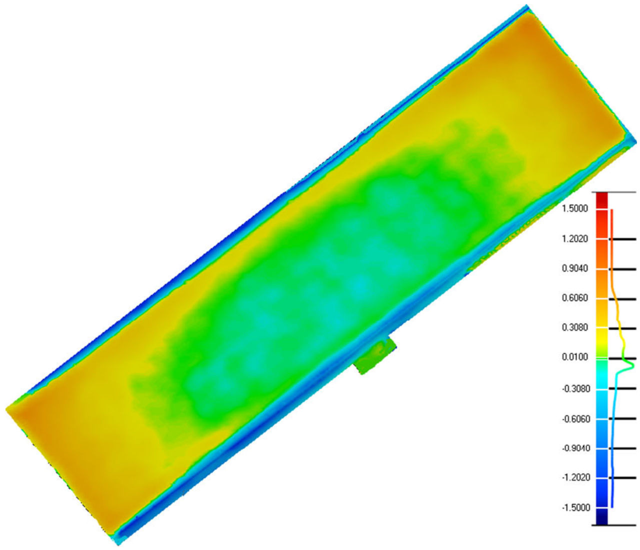

(a) Case 6

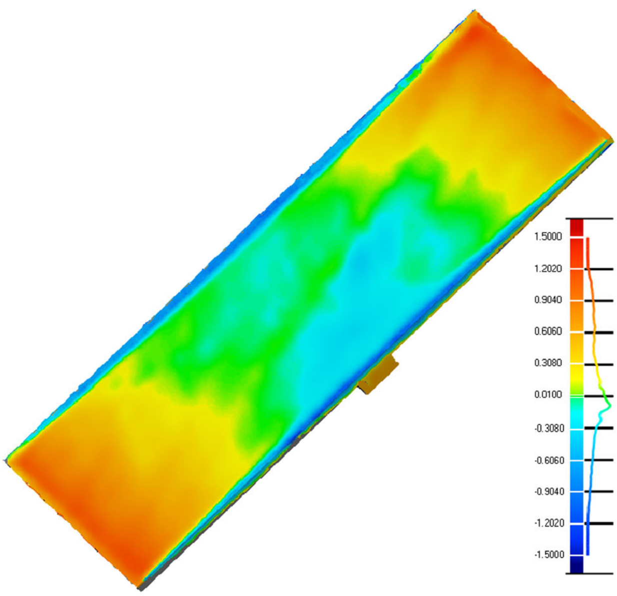

(b) Case 20

Fig. 8 Error cloud chart (unit, mm)

the experimental results indicate that the theoretical model established in Sect. 3.2 can describe the relations between the layer thickness and distortion correctly.

Table 5 Optimum factor level with significant factors and interactions

Factor		A	B	C	D	E
w	Level	1	3	1	3	1
	Value	0.3	110	220	offset raster	0.3

2. As shown in Fig. 8, the biggest distortion of PLA thin-plate part occurs at its four corners, which verifies the validity of theoretical model. It is shown by theoretical model that the dimension of model or part is an important factor for the distortion. Therefore, it should be avoided designing large dimension and thin part in the practical application.
3. The faster the filling speed, the smaller the distortion of PLA thin-plate part, as shown in Fig. 7b. The reason may be that the fast filling speed results in a small range and low-frequency fluctuation of internal stress in the part. However, it is noteworthy that if the filling speed is too fast, the printer will vibrate violently and noise is produced consequently.
4. The low nozzle temperature is helpful to reduce the distortion as shown in Fig. 7c, because the lower nozzle temperature can reduce the temperature gradient during the deposition process when environment temperature is set to a constant. What calls for special attention is that a too low nozzle temperature causes a low liquidity and viscidity of molding material, and this may result in modeling failure.
5. For factor D, the low and medium levels are unidirectional filling style, and the high level is offset filling style. By observing the Fig. 7d, using offset raster causes the smallest distortion followed by short raster.
6. The raster width seems to have little influence on the distortion of PLA thin-plate part as shown in Fig. 7e.

6 Conclusions and future work

In this paper, a theoretical model of PLA thin-plate part distortion in the FDM process was established, and an experimental study was carried out to reveal the distortion mechanism. The special specimen was designed, prepared, and measured. Then, two statistical analysis methods, S/N ratio and ANOVA, were applied to analyze the influence of five factors on the PLA thin-plate part distortion. Finally, the optimal process parameters for PLA thin-plate part in the FDM process were obtained, and the proposed theoretical model was proved efficient.

Ongoing and future work will focus on researching the mechanical properties of PLA thin-plate part in the FDM process. Furthermore, the distortion mechanism of other thermoplastic plastics or other form parts is also an important research for the authors.

Acknowledgments The support of National Natural Science Foundation of China (No. 51475454), Fundamental Research Funds for the Central Universities (No. 2014QNA38), and A Project Funded by the Priority Academic Program Development of Jiangsu Higher Education Institutions in carrying out this research are gratefully acknowledged.

References

1. Chua CK, Leong KF, Lim CS (2010) Rapid prototyping: principles and applications. World Scientific
2. Yan X, Gu P (1996) A review of rapid prototyping technologies and systems. Comput-Aided Des 28(4):307–318
3. Petzold R, Zeilhofer HF, Kalender WA (1999) Rapid prototyping technology in medicine-basics and applications. Comput Med Imaging Graph 23(5):277–284
4. Boschetto A, Giordano V, Veniali F (2012) Modelling micro geometrical profiles in fused deposition process. Int J Adv Manuf Technol 61(9–12):945–956
5. Zein I, Hutmacher DW, Tan KC, Teoh SW (2002) Fused deposition modeling of novel scaffold architectures for tissue engineering application. Biomaterials 23(4):1169–1185
6. Peng A, Xiao XM, Yue R (2014) Process parameter optimization for fused deposition modeling using response surface methodology combined with fuzzy inference system. Int J Adv Manuf Technol 73(1–4):87–100
7. Rutkowski JV, Levin BC (1986) Acrylonitrile-butadiene-styrene copolymers (ABS): Pyrolysis and combustion products and their toxicity-a review of the literature. Fire Mater 10(3–4):93–105
8. Drumright RE, Gruber PR, Henton DE (2000) Polylactic acid technology. Adv Mater 12(23):1841–1846
9. Madhavan NK, Nair NR, John RP (2010) An overview of the recent developments in polylactide (PLA) research. Bioresour Technol 101(22):8493–8501
10. Tymrak BM, Kreiger M, Pearce JM (2014) Mechanical properties of components fabricated with open-source 3-D printers under realistic environmental conditions. Mater Des 58:242–246
11. Kantaros A, Karalekas D (2013) Fiber Bragg grating based investigation of residual strains in ABS parts fabricated by fused deposition modeling process. Mater Des 50:44–50
12. Wang TM, Xi JT, Jin Y (2007) A model research for part warp deformation in the FDM process. Int J Adv Manuf Technol 33(11–12):1087–1096
13. Vatani M, Barazandeh F, Rahimi AR, Nezhad AS (2012) Distortion modeling of SL parts by classical lamination theory. Rapid Prototyp J 18(3):188–193
14. Kim GD, Lee JK (2005) Prediction of curl distortion using classical lamination theory in stereolithography. J Korean Soc Precis Eng 22(11):210–217
15. Yan XR, Yan YN, Zhang RJ, Guo YH (2003) Study on the Interlaminar Stress and Warping Deformation in Laminated Object Manufacturing. Chin J Mech Eng 39(5):36–40
16. Xu HY, Zhang Y, LuB CDY (2004) Numerical simulation of solidified deformation of resin parts in stereolithography rapid protyping. Chin J Mech Eng 40(6):107–112
17. Jayanthi S, Keefe M, Gargiulo EP (1994) Studies in stereolithography: influence of process parameters on curl distortion in photopolymer models. In: Solid Freeform Fabrication Symposium 1994. University of Texas, Austin, 250-258
18. Wiedemann B, Dusel KH, Eschl J (1995) Investigation into the influence of material and process on part distortion. Rapid Prototyp J 1(3):17–22
19. Dalgarno KW, Childs THC, Rowntree I, Rothwell L (1996) Finite element analysis of curl development in the selective laser sintering process. In: Proceedings of the Solid Freeform Fabrication Symposium, 559-566
20. Sonmez FO, Hahn HT (1998) Thermomechanical analysis of the laminated object manufacturing (LOM) process. Rapid Prototyp J 4(1):26–36
21. Nickel AH, Barnett DM, Prinz FB (2001) Thermal stresses and deposition patterns in layered manufacturing. Mater Sci Eng A 317(1): 59–64
22. Zhang Y, Chou K (2008) A parametric study of part distortions in fused deposition modelling using three-dimensional finite element analysis. Proceedings of the Institution of Mechanical Engineers, Part B. J Eng Manuf 222(8):959–968
23. Yugang D, Suqin W, Hao C, Lu BH (2000) Study on the Effect of Photocuring Resin Shrinkage on Parts Curl Distortion in the Process of Laser Rapid Prototyping. Chem Eng (China) 6:013
24. Wanhua Z, Dichen L, Bingheng L (2001) Investigation of the Part Deformation in Stereolithography. J Xi An Jiao Tong Univ 35(7): 705–708
25. Yang HJ, Hwang PJ, Lee SH (2002) A study on shrinkage compensation of the SLS process by using the Taguchi method. Int J Mach Tool Manuf 42(11):1203–1212
26. Mahesh M, Wong YS, Fuh JYH, Loh HT (2004) Benchmarking for comparative evaluation of RP systems and processes. Rapid Prototyp J 10(2):123–135
27. Buchbinder D, Meiners W, Pirch N, Wissenbach K (2014) Investigation on reducing distortion by preheating during manufacture of aluminum components using selective laser melting. J Laser Appl 26(1):012004
28. Youssef HM (2011) Theory of two-temperature thermoelasticity without energy dissipation. J Therm Stresses 34(2):138–146
29. Boley BA, Weiner JH (2012) Theory of thermal stresses. Courier Dover Publications
30. Long S, Atluri SN (2002) A meshless local Petrov-Galerkin method for solving the bending problem of a thin plate. Comput Model Eng Sci 3(1):53–64
31. Sood AK, Equbal A, Toppo V, Ohdarb RK, Mahapatra SS (2012) An investigation on sliding wear of FDM built parts. CIRP J Manuf Sci Technol 5(1):48–54
32. Rayegani F, Onwubolu GC (2014) Fused deposition modelling (FDM) process parameter prediction and optimization using group method for data handling (GMDH) and differential evolution (DE). Int J Adv Manuf Technol 73(1–4):509–519
33. Roy RK (2010) A primer on the Taguchi method. Society of Manufacturing Engineers